Continuum Variations with Luminosity in Accreting X-Ray Pulsars

M.I. Gornostaev[1,2], K.A. Postnov[1,2], D. Klochkov[3], N.I. Shakura[2]

E-mail: *mgornost@gmail.com*

Two-dimensional structure of accretion columns in the radiation-diffusion limit is calculated for two possible geometries (filled and hollow cylinder) for mass accretion rates $\dot{M}$ ranging from 10^{17} to 1.2×10^{18} g s^{-1}. The observed spectral hardening in the transient X-ray pulsars with increasing $\dot{M}$ can be reproduced by a Compton-saturated sidewall emission from optically thick magnetized accretion columns with taking into account the emission reflected from the neutron star atmosphere. At $\dot{M}$ above some critical value $\dot{M}_{cr} \sim (6–8)\times10^{17}$ g s^{-1}, the height of the column becomes such that the contribution of the reflected component to the total emission starts decreasing, which leads to the saturation and even slight decrease of the spectral hardness. Hollow-cylinder columns have a smaller height than the filled-cylinder ones, and the contribution of the reflected component in the total emission does not virtually change with $\dot{M}$ (and hence the hardness of the continuum monotonically increases) up to higher mass accretion rates than $\dot{M}_{cr}$ for the filled columns.

1 Observations

After the discovery of X-ray pulsars in 1971 [1] it was realized that in bright pulsars the radiation plays a crucial role in braking of the accreting matter onto the surface of a neutron star with strong magnetic field. It is now well recognized that once the radiation density above the polar cap starts playing the role in the accreting matter dynamics, an optically thick accretion column above the polar cap is formed [2] (see [3] for the latest investigation). The characteristic height of the column increases with accretion rate, most of the emission escapes through sidewalls, and it can be expected that above some X-ray luminosity the dependence of the observed properties of the continuum emission on the X-ray luminosity can become different from that in the low-luminosity regime.

Indeed, a similar bimodality is observed in the dependence of the X-ray continuum hardness on luminosity. This dependence can be studied using, for example, data from all-sky monitors such as RXTE/ASM and MAXI,

[1] Faculty of Physics, M.V. Lomonosov Moscow State University, Russia
[2] Sternberg Astronomical Institute, Moscow M.V. Lomonosov State University, Russia
[3] Institute of Astronomy and Astrophysics, Karl-Eberhard University, Germany

V. Grinin et al. (eds) Radiation mechanisms of astrophysical objects. Yerevan: Edit Print, 2017, pp. 297–304.

i.e. without dedicated spectroscopic observations which are necessary to measure CRSFs. Following this approach, we measured the hardness ratio as a function of luminosity in the accreting pulsars GX 304–1, 4U 0115+63, V 0332+53, EXO 2030+375, A 0535+26 and MXB 0656–072 using the data from different energy bands of RXTE/ASM. The result is shown in Fig. 1. To convert the ASM count rates into X-ray luminosities, we used published distances to the sources (GX 304–1: ∼2 kpc [4]; 4U 0115+63: ∼7 kpc [5], V 0332+53: ∼7 kpc [6]; EXO 2030+375: ∼7 kpc [7]; A 0535+26: ∼2 kpc [8]; MXB 0656-072: ∼3.9 kpc [9]) and their broadband X-ray spectra from the archival pointed observations with INTEGRAL and RXTE available to us. One can see that at lower fluxes the hardness ratio increases with flux. At a certain flux, however, a flattening of the hardness ratio is observed in 4U 0115+63, V 0332+53, EXO 2030+375, A 0535+26 and MXB 0656–072. This "turnover" occurs at the flux roughly corresponding to luminosities (3–7) × 10^{37} erg s^{-1}. In GX 304–1, which does not show such a turnover, this "critical" luminosity has simply not been reached during the outbursts registered by RXTE/ASM.

A similar dependence of spectral properties on the X-ray flux at luminosities below ∼10^{37} erg s^{-1} was also reported from spectroscopic observations of the transient Be-X-ray pulsar GRO J1008-57 [10].

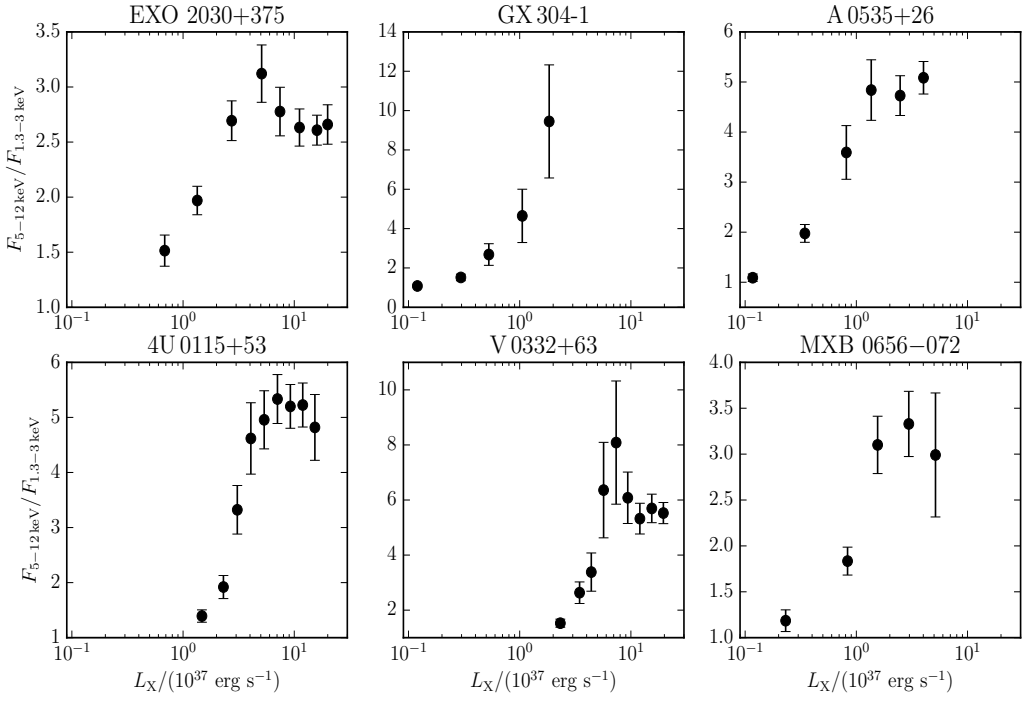

Figure 1: The ratio of the fluxes in 5–12 keV and 1.33–3 keV ranges (referred to as "hardness ratio" in text) measured with RXTE/ASM for six transient accreting pulsars as a function of the total ASM flux in the 1.33–12 keV range.

2 Numerical simulations of accretion column in radiation-diffusion approximation

2.1 Boundary conditions

We introduce cylindrical coordinates r, φ, z centered at the columns axis and $z = 0$ at the neutron star surface. The initial velocity of the falling matter at high altitude above the surface of the neutron star is $v_0 = 10^{10}$ cm s^{-1}. At the cylinder base ($z = 0$), the velocity is $v = 0$. As a boundary condition at the column side surface we used the relation between the radial energy flux and the energy density U in the form $F_r(r_0, z) = 2cU(r_0, z)/3$, which roughly corresponds to the conditions expected in the scattering atmospheres in the Eddington approximation.

2.2 Basic equations

The cylindrical symmetry of the problem makes it essentially two-dimensional. The steady-state momentum equation (ignoring gravity, which is very good approximation as discussed, e.g., in [2]) for accretion braking by the radiation with energy density U reads $(\boldsymbol{S} \cdot \nabla)\, \boldsymbol{v} = -\frac{1}{3}\nabla U$. The mass continuity equation is $\boldsymbol{S} = \rho \boldsymbol{v} = \text{const}$. The integration of momentum equation yields

$$U = 3S(v_0 - v). \tag{1}$$

Following [11], the energy equation can be written as

$$\nabla \cdot \boldsymbol{F} = -\boldsymbol{S} \cdot \nabla \left(\frac{v^2}{2} \right), \tag{2}$$

where we has neglected the flow of internal energy of the falling matter.

The radiative transfer equation for the components of the radiation energy flux in cylindrical coordinates yields

$$F_r = \frac{-\frac{c}{3\varkappa_\perp \rho} \frac{\partial U}{\partial r}}{1 + \frac{1}{3\varkappa_\perp \rho} \frac{1}{U} \left| \frac{\partial U}{\partial r} \right|}, \quad F_z = \frac{-\frac{c}{3\varkappa_\parallel \rho} \frac{\partial U}{\partial z} - \frac{4}{3} U v}{1 + \frac{1}{3\varkappa_\parallel \rho} \frac{1}{U} \left| \frac{\partial U}{\partial z} \right|}, \tag{3}$$

where the denominators are introduced to use the modified diffusion approximation [12].

The system of equations (1)–(3) was solved numerically for accretion rates onto one pole in the range 10^{17}–1.2×10^{18} g s^{-1}for the geometry of filled cylinder with radius r_0 and the hollow cylinder with wall thickness $0.1r_0$ (see [13] for details). The column structure at different accretion rates is shown in Fig. 2.

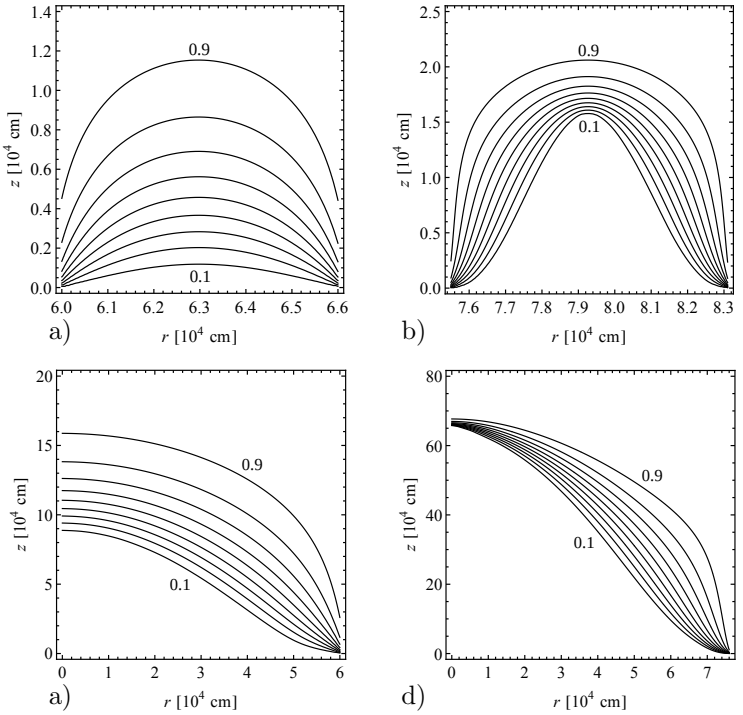

Figure 2: Contours of constant Q (0.9 to 0.1, from top to bottom). The hollow cylinder geometry calculated for $\dot{M}_{17} = 1$ (a) and $\dot{M}_{17} = 5$ (b). The filled cylinder geometry for $\dot{M}_{17} = 1$ (c) and $\dot{M}_{17} = 5$ (d).

3 Hardness ratio variations

3.1 Saturated Compton spectrum of sidewall emission

The LTE treatment of the spectrum of the sidewall emission from accretion columns is clearly a strong oversimplification. To take into account the scattering on electrons in the optically thin boundary of the column, we can use the model calculations of the radiation transfer problem in a semi-infinite plane-parallel atmosphere with strong magnetic field. In this case the emerging spectrum will be formed in the saturated Compton regime, with the mode 1 photons (extraordinary, i.e. polarized perpendicular to the $\boldsymbol{k}-\boldsymbol{B}$-plane, where $\boldsymbol{k}$ is the photon wavevector and $\boldsymbol{B}$ is the magnetic field vector) predominantly escaping through sidewalls [14]. The intensity of mode 2 (ordinary, i.e. polarized in the $\boldsymbol{k}-\boldsymbol{B}$ plane) photons is comparable to that of mode 1 photons only at large angles to the normal, $\mu' \sim 0$, and thus insignificantly contributes to the total flux from the unit surface area due to the geometrical factor.

In this regime, the specific intensity of extraordinary photons at energies far below the cyclotron resonance can be written as $I'_\nu = (1+2\mu')\frac{2\sqrt{3}}{5}\frac{h\nu\nu_g^2}{c^2\tau_0}e^{-\frac{h\nu}{kT}}$ [14], where $\mu' = \cos\theta'$ is the angle between the normal to the atmosphere and the

escaping radiation direction in the plasma reference frame, τ_0 is the characteristic optical depth of the problem, $\nu_g = \frac{eB}{2\pi m_e c}$ is the electron gyrofrequency in the magnetic field. By expressing the characteristic optical depth τ_0 through the emergent radiation flux Φ using (34)–(37) from [14], we find

$$I_\nu = \frac{I'_\nu}{1+2\mu'} = \frac{3}{10\pi}\left(\frac{h\nu}{kT}\right)^2 \frac{\Phi}{\nu} e^{-\frac{h\nu}{kT}}. \tag{4}$$

Therefore, we are in the position to calculate the emerging spectrum from the column in this approximation using the solutions for the column structure obtained above. To do this, it is sufficient to substitute the total radial energy flux at each height of the column $\Phi \to F_r(z)/2$ ($F_r(z)$ in Eq. (3) is known from our numerical calculations), and temperature $T \to T(z)$ estimated deep inside the column (at the optical depth $\sim$1), so that $T(z) = (U(z)/a_r)^{1/4}$.

3.2 Account for the reflected component

Now we should take into account the fact that the electrons in the optically thin part of the column are moving with high velocity $v_0 \sim 1/3c$, and thus the emission beam of the column (4) should be Doppler-boosted towards the neutron star surface and reflected from the neutron star atmosphere, as discussed in [15] and [16]. The reflection coefficient in the case of single Compton electron scattering in strong magnetic field is determined by the ratio $\lambda(\nu) = \kappa_{sc}/(\kappa_{sc} + \kappa_{abs})$, where κ_{sc} and κ_{abs} are the scattering and absorption coefficients for photons in the strong magnetic field, respectively. Since the calculated X-ray albedo turns out to be very similar for both extraordinary and ordinary photons and is virtually insensitive to the photon incident angle to the magnetic field, below we shall use its mode-averaged value for the angle $\pi/4$.

Let α be the angle between the photon wavevector and the plasma bulk velocity vector. The critical value α^* within which the radiation from the height z will be intercepted by the neutron star (in the Schwarzschild metric and with taking into account the difference between the polar axis and the column cylinder side) is

$$\alpha^*(z) = \arcsin\left(\frac{R_{NS}}{\sqrt{(R_{NS}+z)^2+r_0^2}}\sqrt{\frac{1-r_S/\sqrt{(R_{NS}+z)^2+r_0^2}}{1-r_S/R_{NS}}}\right) - \arctan\frac{r_0}{R_{NS}+z},$$

where $r_S = 2GM/c^2$ is the Schwarzschild radius (cf. [16]).

Let Σ be the surface of the column, $\Sigma'(\varphi, z)$ be a point on the surface and $d\Sigma = r_0 d\varphi dz$ be the elementary area. The flux from the surface element at frequency ν (in conventional notations) reads $f_\nu(\Sigma') = dE(\Sigma')/(dtd\nu d\Sigma)$ and can be separated into three parts in accordance to the angle relative to the observer. Photons escaping with angles $\alpha > \alpha^*$ to the column are directly seen as the proper column radiation f_ν^{col}. The second part includes the radiation f_ν^{ref} intercepted by the neutron star and reflected from the neutron star surface with

X-ray albedo $\lambda(\nu)$. The third part f_ν^{abs} is the radiation absorbed and re-radiated by the neutron star atmosphere. Then we can write

$$\begin{aligned} f_\nu(\Sigma') &= \int\limits_{-1}^{1} \frac{df_\nu(\Sigma')}{d\cos\alpha} d\cos\alpha \\ &= \int\limits_{-1}^{\cos\alpha^*} \frac{df_\nu(\Sigma')}{d\cos\alpha} d\cos\alpha + \lambda(\nu) \int\limits_{\cos\alpha^*}^{1} \frac{df_\nu(\Sigma')}{d\cos\alpha} d\cos\alpha + (1-\lambda(\nu)) \int\limits_{\cos\alpha^*}^{1} \frac{df_\nu(\Sigma')}{d\cos\alpha} d\cos\alpha \\ &= f_\nu^{col}(\Sigma') + f_\nu^{ref}(\Sigma') + f_\nu^{abs}(\Sigma'). \end{aligned} \tag{5}$$

The integrands [16] in the cylindrical coordinates with account for the axial symmetry ($I_\nu(\Sigma') = I_\nu(z)$, giving by (4)) have the form

$$\frac{df_\nu(\Sigma')}{d\cos\alpha} = I_\nu(z) \frac{2D^3}{\gamma} \sin\alpha \left(1 + \frac{\pi D}{2} \sin\alpha\right),$$

where the Doppler factor is $D = 1/(\gamma(1 - \beta\cos\alpha))$, $\gamma = 1/\sqrt{1-\beta^2}$ is the plasma Lorentz factor and $\beta = v/c$. Then for the total radiation from the column at frequency ν we obtain

$$\begin{aligned} L_\nu &= \iint\limits_{\Sigma} f_\nu(\Sigma') d\Sigma = 2\pi r_0 \int\limits_0^{z_{max}} \left(f_\nu^{col}(z) + f_\nu^{ref}(z) + f_\nu^{abs}(z)\right) dz \\ &= L_\nu^{col} + L_\nu^{ref} + L_\nu^{abs}, \end{aligned} \tag{6}$$

where z_{max} is the upper limit of the computational area. The observed X-ray flux from one column is $F_\nu = (L_\nu^{col} + L_\nu^{ref})/(4\pi d^2)$, where d is the distance to the source. For the illustrative purposes, we assume $d = 5$ kpc. Taking into account the radiation absorbed by the neutron star atmosphere L_ν^{abs} will add more soft photons to the total spectrum.

Since we are observing both the direct and reflected radiation from the column, the total change in the hardness of the spectrum depends on the fraction of the reflected radiation in the total flux. This, in turn, depends on the height of the column. We have calculated the total flux as the sum of the direct and reflected component as a function of $\dot{M}$ with taking into account the photon ray propagation in the Schwarzschild metric of the neutron star with a fiducial mass $M = 1.5M_\odot$ and radius $R = 10$ and 13 km. The magnetic field of the neutron star is set to 3×10^{12} G, so that the CRSF energy is about 35 keV. The result is presented in Fig. 3. It is seen that the hardness ratio

$$\mathrm{HR} = \int\limits_{5\ \mathrm{keV}}^{12\ \mathrm{keV}} F_\nu d\nu \Bigg/ \int\limits_{1.3\ \mathrm{keV}}^{3\ \mathrm{keV}} F_\nu d\nu$$

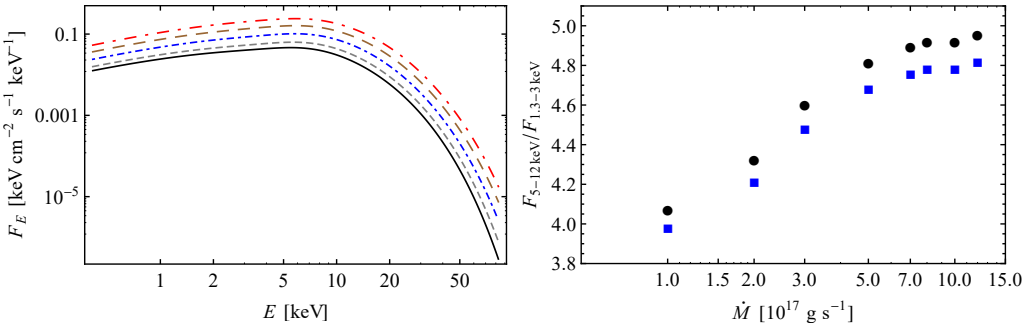

Figure 3: *Left:* the total spectrum of direct sidewall and reflected from the neutron star atmosphere from the optically thick filled accretion column for mass accretion rates $\dot{M}_{17} = 2$, 3, 5, 8 and 12 (from bottom to up, respectively). *Right:* the hardness ratio HR of the total spectrum. Shown are calculations for the neutron star radius $R_{NS} = 10$ km (squares) and $R_{NS} = 13$ km (circles).

first increases with the mass accretion rate (X-ray luminosity), but starting from $\dot{M}_{cr} \sim (6-8)\times 10^{17}$ g s^{-1}, it gets saturated. This is in agreement with observations shown in Fig. 1.

For the hollow cylinder accretion columns which have smaller height (see Fig. 2), the fraction of the reflected component in the total emission does not virtually change with mass accretion rate within the calculated range, therefore the hardness ratio of the total spectrum monotonically increases with $\dot{M}$ in this range. Note also that in this case the spectrum is harder than in the case of the filled column because the reflected (harder) emission dominates in the total spectrum.

4 Summary and conclusions

Therefore, our model calculations lead to the following conclusions:

1. The spectral hardening in X-ray pulsars with positive CRSF energy dependence on X-ray flux can be explained by increasing of the Comptonization parameter y in the slab atmosphere of the accretion mound. It is in this regime that positive correlation of the cyclotron line is observed, for example, in Her X-1 [17].
2. At high accretion rates, the radiation-supported optically thick accretion column grows above the polar cap, the sidewall emission from the column is formed by extraordinary photons in the saturated Compton regime. The spectrum of this emission gets harder with increasing mass accretion rate.
3. With further increasing mass accretion rate the height of the column increases, such that the fraction of radiation reflected from the neutron star atmosphere starts decreasing. As the reflected radiation is harder than the incident one,

the spectrum of the total emission (direct plus reflected) stops hardening (and even becomes slightly softer).

4. In the frame of this model, the saturation of the spectral hardness in the case of a hollow cylinder geometry of the accretion column can be achieved at much higher accretion rates (roughly, scaled with the relative thickness of the column wall, b), because the characteristic height of the column in this case is correspondingly smaller than that of the filled column.

References

1. *R. Giacconi, H. Gursky, E. Kellogg et al.*, Astrophys. J. Lett., **167**, L67, 1971.
2. *M.M. Basko, R.A. Sunyaev*, Mon. Not. Roy. Astron. Soc., **175**, 395, 1976.
3. *A.A. Mushtukov, V.F. Suleimanov, S.S. Tsygankov, J. Poutanen*, Mon. Not. Roy. Astron. Soc., **447**, 1847, 2015.
4. *G.E. Parkes, P.G. Murdin, K.O. Mason*, Mon. Not. Roy. Astron. Soc., **190**, 537, 1980.
5. *I. Negueruela, A.T. Okazaki*, Astron. Astrophys., **369**, 108, 2001.
6. *I. Negueruela, P. Roche, J. Fabregat, M.J. Coe*, Mon. Not. Roy. Astron. Soc., **307**, 695, 1999.
7. *C.A. Wilson, M.H. Finger, M.J. Coe et al.*, Astrophys. J., **570**, 287, 2002.
8. *I.A. Steele, I. Negueruela, M.J. Coe, P. Roche*, Mon. Not. Roy. Astron. Soc., **297**, L5, 1998.
9. *V.A. McBride, J. Wilms, M.J. Coe et al.*, Astron. Astrophys., **451**, 267, 2006.
10. *M. Kühnel, S. Müller, I. Kreykenbohm et al.*, Phys. J. Web Conf., **64**, 6003, 2014.
11. *K. Davidson*, Science, **246**, 1, 1973.
12. *Y.-M. Wang, J. Frank*, Astron. Astrophys., **93**, 255, 1981.
13. *K.A. Postnov, M.I. Gornostaev, D. Klochkov et al.*, Mon. Not. Roy. Astron. Soc., **452**, 1601, 2015.
14. *Y.E. Lyubarskii*, Astrophys., **25**, 577, 1986.
15. *Y.E. Lyubarskii, R.A. Syunyaev*, Astron. Lett., **14**, 390, 1988.
16. *J. Poutanen, A.A. Mushtukov, V.F. Suleimanov et al.*, Astrophys. J., **777**, 115, 2013.
17. *R. Staubert, N.I. Shakura, K. Postnov et al.*, Astron. Astrophys., **465**, L25, 2007.

* The color figures are available online in the Proceedings at *http://www.astro.spbu.ru/sobolev100/*.